Use of SPOT HRV Data in the Corps of Engineers Dredging Program

Carolyn J. Merry, Harlan L. McKim, and *Nancy LaPotin*
U.S. Army Cold Regions Research and Engineering Laboratory, 72 Lyme Road, Hanover, NH 03755-1290
John R. Adams
U.S. Army Engineer District, Buffalo, 1776 Niagara Street, Buffalo, NY 14207-3199

ABSTRACT: The Corps of Engineers coordinated a water quality sampling program with a dredged material disposal operation and a concurrent SPOT overpass on 4 June 1986. The SPOT HRV 20-m multispectral data were classified into five water categories using a maximum likelihood classifier. A post-classification filter was used to smooth the water. Due to the limited amount of ground truth data, simple empirical models are presented to illustrate the association between turbidity and spectral class.

INTRODUCTION

THE CORPS OF ENGINEERS has a wide variety of water-related mission responsibilities, but one of the most important is navigation. There are 25,000 miles of navigable inland waterways in the United States. The barge traffic on these waterways transports millions of dollars worth of commerical goods annually. The Corps is responsible for keeping these waterways open. In addition, the Corps must keep navigation channels open in nearshore and estuarine environments by dredging these channels and maintaining them, in many cases, at a minimum channel depth of 35 to 40 ft.

As a result of these dredging operations, there are millions of tons of material that must be disposed of on the land, in nearshore environments, or in the ocean. The dredged material from many locations can be used beneficially for beach nourishment projects and for developing waterfowl and fishery habitats. When the material dredged contains pollutants that could be harmful to human and aquatic life, other techniques, such as containment facilities, must be used when disposing of it.

In areas where the impact of unconfined disposal of dredged material must be monitored, the cost of site selection and subsequent water quality monitoring can become very high. It is important in these instances to select representative water quality sampling locations, but it is equally important to minimize the number of water quality samples required.

With this in mind, a study was done to (1) review the application of existing remote sensing techniques for providing data in the Corps' dredging program, (2) define promising new remote sensing techniques for monitoring and managing dredged disposal sites, and (3) recommend which remote sensing techniques should be used now and which techniques should be developed for the future (McKim *et al.*, 1985). It was found that additional research is required to study the use of multispectral scanners for bathymetric mapping of large coastal areas, for mapping sediment transport in shallow waters, for mapping concentrations of suspended matter of organic or inorganic origin, and for detecting vegetative stress and soil properties (McKim *et al.*, 1985). Along with acquiring multispectral data, ground truth needs to be taken to verify the interpretation of the data.

The spatial resolution and time frequency of data acquisition are important when evaluating remote sensing techniques for use in the dredging program. The French Système Probatoire d'Observation de la Terre (SPOT) satellite system is the first operational system that will allow data acquisition and distribution in a short time frame (less than 48 hrs). Initially, the SPOT high resolution and pointable system was evaluated as a means of collecting water quality data that would augment and potentially reduce the conventional data collection activities of the Corps and the state of Maryland at the Hart-Miller Island disposal area (Band *et al.*, 1984). The research begun at Hart-Miller Island has been continued for the dredging operation in the Toledo Harbor, Ohio area. This paper reports on the study completed for Toledo Harbor.

DESCRIPTION OF THE SPOT SATELLITE SYSTEM

The French SPOT satellite, launched on 21 February 1986, is in a sun-synchronous, near-polar orbit. For any given region, the satellite images the Earth at the same local time on consecutive passes. In its nominal orbit at 832-km altitude, the SPOT satellite crosses the Equator during its descending node at about 1030 local time. The satellite's motion is also synchronized with the daily rotation of the Earth so that the pattern of successive ground tracks is repeated at 26-day intervals.

The sensor package consists of two High Resolution Visible (HRV) sensors. The HRV is a "push-broom" scanner, which means it images a complete line of the ground scene in the cross-track direction in one "look" without any mechanical scanning. The instrument is also pointable and can image an area on the ground $\pm 27°$ from nadir. When the satellite is pointed at nadir, the HRVs each image adjacent 60-km ground areas. There is a 3-km overlap in the center, for a total image width of 117 km.

The satellite can point off to either side of nadir at 0.6° increments and can thus image any area within a 950-km swath centered over the orbital path. This allows for stereo acquisition of imagery and for more revisit opportunities over an area of interest than is possible with the Landsat series. For example, at the latitude of 42°N for Hanover, New Hampshire, the sensor could image an area 11 times during a 26-day orbital cycle. A maximum of six stereo-pairs can also be obtained during the 26-day cycle.

The data are of high radiometric quality with 8-bit resolution for 256 radiometric levels. There are two modes of instrument operation: multispectral and panchromatic. The 20-m multispectral mode covers three spectral regions – two in the visible (0.50 to 0.59 μm, 0.61 to 0.68 μm) and one in the near infrared (0.79 to 0.89 μm). The 10-m panchromatic mode covers a wide band ranging from 0.51 to 0.73 μm. Additional details on the SPOT satellite system can be found in Begni (1982), Begni *et al.* (1984), Chevrel *et al.* (1981), and CNES (1982).

In this paper we address the possibility of using the off-nadir viewing capability with 20-m multispectral data for mapping relative ranges of suspended sediment concentration associated with a Corps dredged material disposal operation.

PHOTOGRAMMETRIC ENGINEERING AND REMOTE SENSING,
Vol. 54, No. 9, September 1988, pp. 1295–1299.

0099-1112/88/5409–1295$02.25/0

GROUND TRUTH DATA ACQUISITION

The Buffalo District, Corps of Engineers, conducted a monitoring program during the summer of 1986 to study the effects of open-lake disposal operations on the water quality of Lake Erie. The dredged material disposal area is located northeast of Toledo, Ohio, and is within the rectangle located southeast of the navigation channel (Figure 1).

The dredged material disposal operation occurred over a period of 14 weeks, starting on 7 April and ending on 8 June 1986. *In situ* measurements of water quality were taken twice before the dredging operation began on 7 April. Water quality measurements were then made every week until 18 June 1986, including two measurement sets after dredging ceased on 8 June 1986.

A programming request was made of SPOT IMAGE Corporation to obtain SPOT HRV data over the Toledo area during the Corps dredging operation. The District's water quality sampling program was readjusted to coordinate with a dredged disposal operation and a SPOT overpass on 4 June 1986. As a result, a completely cloud free SPOT image was acquired successfully on 4 June at 1242 hrs (DST).

The water quality data taken on 4 June are shown in Table 1, with the location of the water quality sampling stations shown in Figure 2. Seventy percent of the dredged material disposed during the 4 June operation was clay.

TABLE 1. MEASUREMENTS FROM THE WATER QUALITY STATIONS LOCATED NEAR THE DREDGED DISPOSAL SITE AT THE TIME OF THE SPOT OVERPASS.

Location no.	Suspended sediment (mg/L)*	Turbidity (NTU)†	Secchi depth (ft)
1	2.0	19.0	2.0
2	2.0	7.3	2.5
3	2.0	6.8	2.5
4	7.0	26.0	2.0
5	5.0	18.0	2.5
6	<1.0	7.9	2.5
7	<1.0	8.3	3.0
8	8.0	23.0	2.0
9	3.0	20.0	2.5
10	2.0	20.0	2.5
11	1.0	6.1	3.0
12	1.0	5.7	3.0
13	6.0	7.5	3.5

*The measurement accuracy of the suspended load concentration for the sampling procedure used by the District is ±2 mg/L.
†NTU = Nephelometric Turbidity Units

ANALYSIS OF THE SPOT HRV DATA

MATCHING THE IMAGE TO THE MAP

The SPOT HRV data set was analyzed on a Dipix ARIES-II image processing system. The HRV image was registered to a NOAA map sheet (scale 1:40,000) using an Altek digitizing table and Gentian controller interfaced to the image processing system. The navigation channel and the location of the water quality sampling stations were located, digitized, and stored as overlay theme files on the SPOT image.

Interpretive analysis of the digital count values for the entire SPOT scene indicated that there were from five to seven different water types in the area of interest. Using this information as a guideline, a 723- by 670-pixel subarea (approximately 14 km on a side) that contained the dredged material disposal area was selected from the HRV image for analysis.

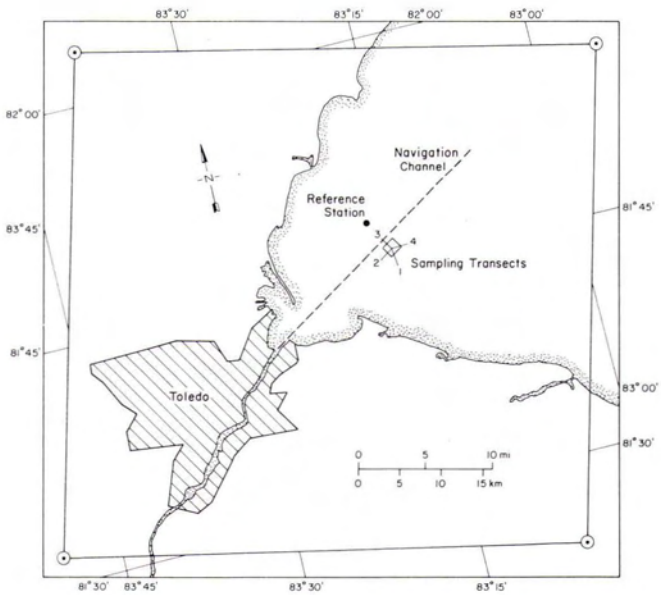

FIG. 1. Site location map of the study area.

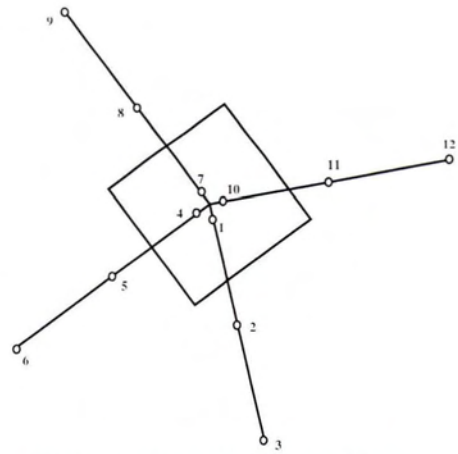

FIG. 2. Location map of the water quality sampling stations.

UNSUPERVISED CLASSIFICATION OF DATA

An unsupervised maximum likelihood classification was performed on the subarea. The classifier delineates "equiprobability contours," shown as ellipsoids for two spectral bands (Figure 3). A normal probability density function is calculated for each of these ellipsoids, which are also characterized by a mean vector and a covariance matrix. The shape of these equiprobability contours shows the sensitivity of the maximum likelihood classifier. The probability density function is used to classify an unknown pixel by computing the probability of a pixel belonging to each of the categories. After the probabilities are evaluated, the pixel is assigned to the most likely class.

The unsupervised classification procedure of the ARIES-II software generates n-dimensional histograms, with the n dimensions in this case representing the three SPOT spectral

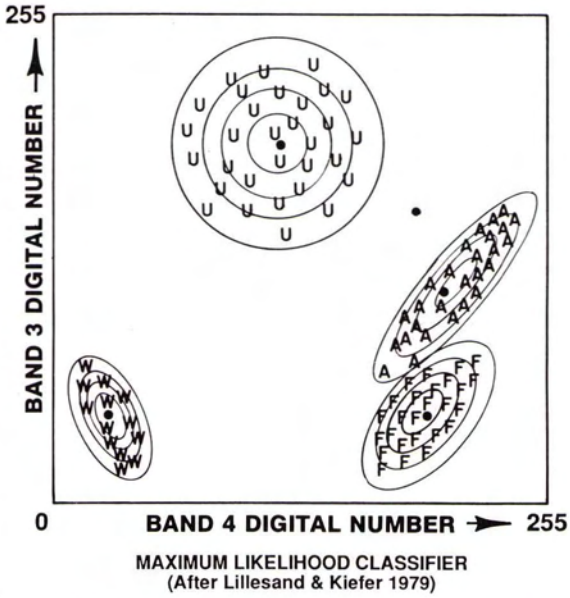

FIG. 3. Schematic of maximum likelihood classifier. For example, the letters (W, U, C, H, F) are clusters of pixels, each representing a unique spectral response. (After Lillesand and Kiefer, 1979.)

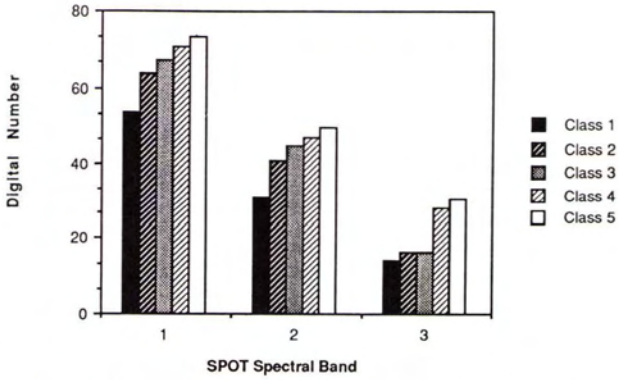

FIG. 4. Mean values of the five multispectral signatures.

bands, and searches for maximum values within each histogram. There were 17 maximum histogram peaks generated for the three-band data. The range of values used in the histogram generation process was limited to the range of the histogram values within each band. An equal number of pixels per histogram bin was allocated so than an equal number of bins represented each band. The 17 maxima were then merged into five multiple parallelepiped classes to create Gaussian multispectral signatures. A maximum likelihood classification was performed on the data set using these five spectral signatures.

The mean values of the five multispectral signatures show than the digital count values increase from class 1 to class 5 for each spectral band (Figure 4). Spectral class 1 (pink) was the least reflective water, and spectral class 5 (green) contained the most reflective water. The basis for this interpretation is that in pure water the attenuation of light is dominated by the absorption of water below wavelengths of 0.3 μm and above 0.7 μm (Morel, 1974). The presence of particulate and dissolved material in the water will affect the penetration of light in water and the intensity and color of the light scattered back in the direction of the remote sensor (Philpot and Klemas, 1979). Because spectral class 1 had the lowest values for all three bands and spectral class 5 the highest values (see Figure 4), then spectral class 5 contained the greatest suspended sediment load.

There were many unclassified pixels in the initial water classification. Therefore, post-classification filtering was performed on the classification map. The filtering algorithm is based on the minimum area of a homogeneous theme, seven pixels in this case (Dipix Systems Limited, 1986). Results from the smoothing algorithm showed that the water classification was not affected significantly. The differences between the "before" and "after" maps of the areal distribution of each class were less than 2 percent, as shown in Table 2.

MATCHING THE IMAGE DATA TO THE WATER QUALITY DATA

To correlate the water quality data at the 13 stations with the spectral class information, the overlay of the water quality sampling locations was superimposed on the water classification map (Plate 1). The water quality data from the 13 locations were analyzed next. Sampling point 13 represents the District's reference sampling location and is considered an outlier.* The strongest correlation between the water quality data shown in Table 1 and the spectral classes was found with the turbidity (measured in NTUs), which is a measure of light scattering. However, a quantitative measure of suspended load is normally expressed in mass per unit volume or concentration (mg/L). To obtain the relationship between the concentration and the spectral class, two models were developed. The first model related the turbidity level (in NTUs) to the suspended sediment concentration (in mg/L) and the second model related the turbidity (measured in NTU) to the spectral classification index (from class 1 to 5).

Figure 5 shows an exponential model correlating the suspended sediment with the turbidity. The equation for model 1 is shown below:

$$y = (0.511)\,(10^{0.042x}) \qquad (1)$$

$$<0.01005> \qquad \{4.15908\} \qquad (0.002)$$

where y = suspended sediment concentration (mg/L),
x = turbidity (NTU),
$< >$ = standard error of estimate,
$\{\}$ = t statistic, and
$(\,)$ = p-value for t statistic.

Table 3 shows the ANOVA table for Equation 1. The residuals

TABLE 2. CLASSIFICATION SUMMARY STATISTICS FOR THE NON-FILTERED AND FILTERED WATER CLASSIFICATIONS.

	Non-filtered		Filtered		
Class no.	Pixels (no.)	Total (%)	Pixels (no.)	Total (%)	Deviation (%)
1 (pink)	27268	5.6	24259	5.0	−0.6
2 (yellow)	245565	50.6	254125	52.3	1.7
3 (red)	151480	31.2	149359	30.7	−0.5
4 (blue)	43370	8.9	41009	8.4	−0.5
5 (green)	16586	3.4	17043	3.5	0.1
Unclassified	1535	0.3	9	0.1	−0.2
Total	485804	100.0	485804	100.0	0.0

*The suspended sediment concentration for point 13 is high in comparison to the other data (6.0 mg/L), the turbidity value is low (7.5 NTU), but the secchi disk depth is high (measuring 3.5 ft), which is inconsistent with the other 12 data values (see Figure 5 and Table 1). Also, the spectral values for point 13 were examined in each band to check for inconsistencies and were found to be representative for spectral class 2. This implies a probable measurement error with point 13, perhaps resulting from the relatively low concentrations of suspended sediment (ranging from <1.0 to 8.0 mg/L).

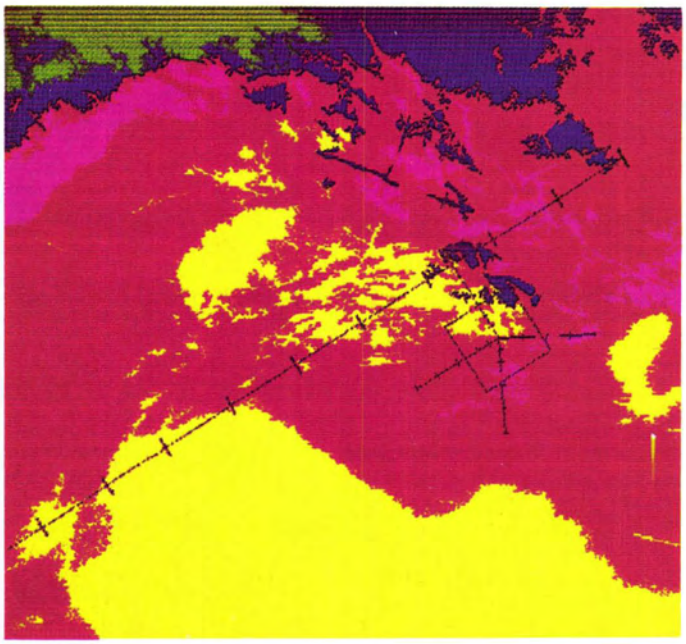

PLATE 1. Water sampling transects and navigation channel overlaid on the water classification map.

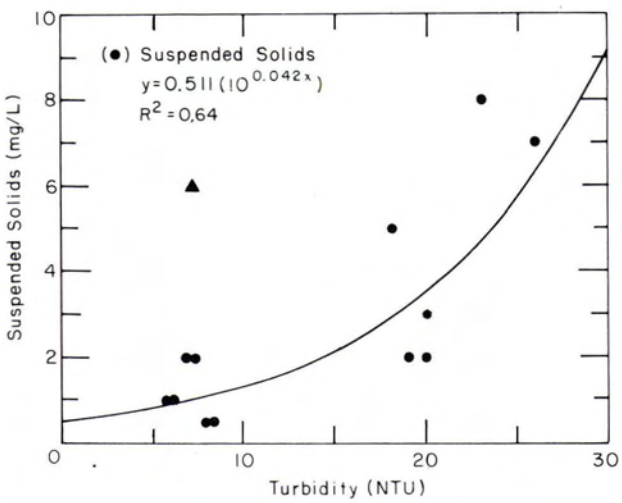

FIG. 5. Exponential model relating suspended sediment concentration to turbidity.

are symmetric around zero with no outliers (Figure 6). About 64 percent of the variance in suspended sediment concentration is explained by using the turbidity value as an indicator. The standard error of the model is 0.01 mg/L†.

Figure 7 shows the model developed relating the spectral class to the turbidity level. The relationship was logarithmic of the form

$$\begin{array}{ll} y & = (1.171)(x^{0.306}) \\ <0.09284> & \quad \{3.29805\} \\ & \quad\quad (0.008) \end{array} \qquad (2)$$

where y = spectral class (from 1 to 5),
x = turbidity (NTU),

†The measurement accuracy of the suspended load concentration for the sampling procedure used by the District is ±2 mg/L.

TABLE 3. ANOVA TABLE FOR EQUATION 1.

Source	Sum of Squares	Deg. of Freedom	Mean Squares	F-Ratio	Prob >F
Model	1.111	1	1.111	17.298	0.002
Error	0.642	10	0.064		
Total	1.753	11			

Coefficient of determination: 0.635
Standard error of estimate: 0.253
Spearmans corr. (suspended solids, turbidity): 0.597; p = 0.031

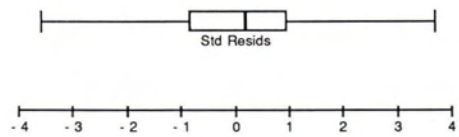

FIG. 6. Schematic plot of the residuals for the exponential model shown in Equation 1.

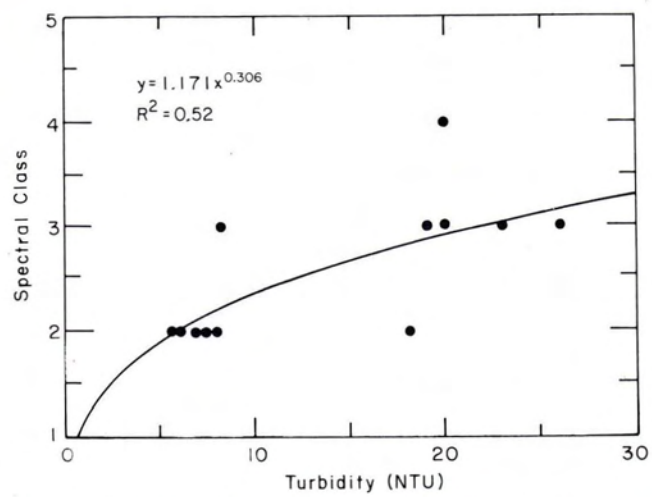

FIG. 7. Logarithmic model relating spectral classification to turbidity level.

< > = standard error of estimate,
{ } = t statistic, and
( ) = p-value for t statistic.

Table 4 shows the ANOVA table for Equation 2. The residuals are symmetric around zero with three outliers (Figure 8).

The coefficient of determination for the model is 0.52, suggesting that 52 percent of the variation in spectral class definition is explained by using the turbidity value as an indicator. The model illustrates the non-linear association between turbidity and spectral class; however, it should be used solely as an illustrative model due to the small sample size (12). A non-linear model, rather than a linear model, was the best-fit model that related turbidity with the index values of spectral class.

SUMMARY AND CONCLUSIONS

The results from the study indicate that the 20-m multispectral data from the SPOT satellite is useful for differentiating between relative suspended sediment levels at dredged disposal areas. Around the immediate dredged disposal area, very little variation was seen in the water quality sampling data. The sparsely sampled ground truth data and the 2-mg/L measurement accuracy did not warrant a complete statistical analysis of the digital image data. The first model showed a nonlinear as-

TABLE 4. ANOVA TABLE FOR EQUATION 2.

Source	Sum of Squares	Deg. of Free-dom	Mean Squares	F-Ratio	Prob >F
Model	0.357	1	0.357	10.877	0.008
Error	0.328	10	0.032		
Total	0.68570	11			

Coefficient of determination: 0521
Standard error of estimate: 0181
Spearmans corr. (spectral class, turbidity): 0.807; p = 0.001
Kruskal-Wallis one-way nonparametric ANOVA: 8.188; p = 0.017

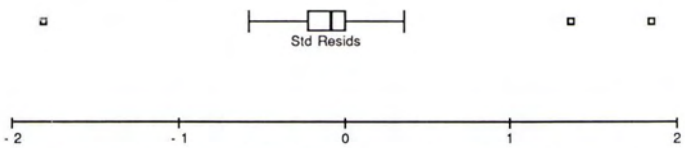

FIG. 8. Schematic plot of the residuals for the logarithmic model shown in Equation 2.

sociation between suspended sediment concentration and turbidity. The highest nonparametric correlation (0.807) for spectral class separation was with the turbidity value (in NTUs) for low levels of suspended sediment.

Future efforts should include measurements at both surface and non-surface points. In addition, algorithms need to be developed to relate surface measurements to sub-surface concentration profiles and spatially distribute this information across the test area. Provided that an adequate sample size is obtained, equations of the form (1) and (2) might be helpful for correlating SPOT image data to water quality sampling and other ground truth measures.

Because of the small amount of field data available from the study, another test will be done in the future. Near-real-time remotely sensed information, such as the NOAA Advanced Very High Resolution Radiometer (AVHRR) imagery, will be used to select areas of Lake Erie for positioning the water quality sampling transects. Additional point data will be collected over a wider range of turbidity or suspended sediment concentration data. These measurements will be made over the entire water column as determined by the secchi depth measurement. This will allow comparison with the data collected in June 1986.

ACKNOWLEDGMENTS

The work was sponsored under the Corps of Engineers Civil Works Remote Sensing Research Program, CWIS 31746, Evaluation of SPOT and Landsat-4 Satellite Data Products, and reimbursable orders from the Buffalo District, Corps of Engineers and the Water Resources Support Center, Dredging Division (WRSC-D). Appreciation is extended to Eleanore Meredith (SPOT IMAGE Corporation) for her help in coordinating with SPOT IMAGE to acquire the satellite image during our water quality sampling program, to Charles Hummer (WRSC-D) for his support of our research with SPOT HRV data for application to the Corps Dredging Program, to Perry J. LaPotin for helpful technical discussions, and to Richard Birnie (Dartmouth College), Stephen Yaksich (Buffalo District, Corps of Engineers), and Andrew J. Bruzewicz (Rock Island District, Corps of Engineers) for technical review of this report.

REFERENCES

Band, L.E., H.L. McKim, and C.J. Merry, 1984. The potential use of SPOT HRV imagery for analysis of coastal sediment plumes, SPOT Simulation Applications Handbook, *Proceedings of the 1984 SPOT Symposium*, 20-23 May, Scottsdale, Arizona, pp. 199-204.

Begni, G., (1982). Selection of the optimum spectral bands for the SPOT satellite, *Photogrammetric Engineering and Remote Sensing*, Vol. 48, No. 10, pp. 1613–1620.

Begni, G., D. Leger, and M. Dinguirard, 1984. An in-flight refocusing method for the SPOT HRV cameras, *Photogrammetric Engineering and Remote Sensing*, Vol. 50, No. 12, pp. 1697–1705.

Chevrel, M., M. Courtois, and G. Weill, 1981. The SPOT satellite remote sensing mission, *Photogrammetric Engineering and Remote Sensing*, Vol. 47, No. 8, pp. 1163–1171.

CNES, 1982. *SPOT Satellite-Based Remote Sensing System*, CNES: Paris, France.

Dipix Systems Limited, 1986. *ARIES System User's Manual.*

Lillesand, T.M., and R.W. Kiefer, 1987. *Remote Sensing and Image Interpretation*, John Wiley & Sons, Inc.: New York, New York.

McKim, H.L., V. Klemas, L.W. Gatto, and C.J. Merry, 1985. *Potential of Remote Sensing in the Corps of Engineers Dredging Program*, CRREL Special Report 85–20, 47 p.

Morel, A., 1974. Optical properties of pure water and pure sea water, *Optical Aspects of Oceanography* (Jerlov and Nielsen, eds.), Academic Press: New York.

Philpot, W., and V. Klemas, 1979. *The Use of Satellites in Environmental Monitoring of Coastal Waters*, Final Report, CRS-1–80, NASA Langley Research Center: Hamptom, Virginia.

(Received 25 January 1988; accepted 19 April 1988; revised 31 May 1988)

Short Course
Desktop Mapping with SPOT Image Data

University of Georgia, Athens, Georgia
9–11 November 1988

The Center for Remote Sensing and Mapping Science (CRMS), University of Georgia, and SPOT Image Corporation, Reston, Virginia have announced a short course, Desktop Mapping with SPOT Image Data, that will feature instruction in digital image processing for mapping and geographic information system (GIS) applications. The course will include a series of lectures and hands-on exercises designed to acquaint participants with satellite image data recorded by the SPOT HRV sensors in panchromatic (10-m) and multispectral (20-m) formats, and the use of the powerful Desktop Mapping System (DMS), an inexpensive personal computer software package for producing planimetric, thematic, topographic, and GIS products from digital image data.

For further information please contact

Dr. Roy Welch, Director
Center for Remote Sensing and Mapping Science
Department of Geography
University of Georgia
Athens, GA 30602
Tele. (404) 542-2856